



ELSEVIER

Optics and Lasers in Engineering 37 (2002) 159–170

---

---

OPTICS and LASERS  
in  
ENGINEERING

---

---

# Frequency conversion in novel materials and its application to high resolution gas sensing

Ady Arie\*, Keren Fradkin-Kashi, Yonatan Shreberk

*Department of Electrical Engineering, Physical Electronics, Faculty of Engineering, Tel-Aviv University, Tel-Aviv 69978, Israel*

Received 9 April 2001; received in revised form 14 May 2001; accepted 15 May 2001

---

## Abstract

We have constructed a compact room-temperature mid-infrared spectrometer and gas sensor, based on quasi-phase matched difference-frequency generation in periodically poled ferroelectric crystals of the  $\text{KTiOPO}_4$  family, namely:  $\text{KTiOPO}_4$ ,  $\text{KTiOAsO}_4$  and  $\text{RbTiOAsO}_4$ . The wide tunability of the spectrometer ( $3.1\text{--}3.75\ \mu\text{m}$ ) enables us to cover an entire vibrational band of gases such as methane and nitrous oxide. The high spectral resolution ( $\sim 1\ \text{MHz}$ ) is used to investigate the spectral profile of the hyperfine components of a single rotational transition. The sensitivity of the described spectrometer is  $\sim 75$  parts per million. Applications of this technology include the detection of polluting or toxic gases, biomedical sensing, atmospheric research, volcanic monitoring and industrial process control. © 2002 Elsevier Science Ltd. All rights reserved.

*Keywords:* Optical sensor; Laser

---

## 1. Introduction

There is considerable interest in developing sensitive yet robust and compact techniques for the detection of environmentally important gases and pollutants. The fundamental vibrational transitions of most molecules lie in the  $2\text{--}20\ \mu\text{m}$  wavelength region. Each material can be characterized by its unique ‘fingerprint’ absorption spectrum, thus mid-infrared (mid-IR) optical spectroscopy provides a convenient real-time method for the detection and discrimination of gases. This technique can also be used for quantitative measurements of gas concentrations, even in the

---

\*Corresponding author. Tel.: +972-3-640-6627; fax: +972-3-642-3508.

*E-mail address:* ady@eng.tau.ac.il (A. Arie).

presence of undesirable background gases. Mid-IR spectroscopy has many applications, including: industrial process control applications, analysis of gas emissions from automobiles, air quality monitoring in confined environments, atmospheric chemistry, volcanic research, biomedical applications etc.

While high sensitivity and improved spectral resolution are provided by coherent light sources, only few suitable laser sources currently exist in the mid-infrared range. Lead-salt lasers are usually multimode, require low temperature for CW operation, and often suffer from mode-hops during tuning. Several gas lasers also emit in the mid-IR range, but they are not continuously tunable and have large dimensions compared to solid state lasers. Recently, distributed feedback quantum cascade lasers were proposed as a promising technology for coherent radiation sources in the mid-IR range, but presently, they still also require cooling to low temperature for CW operation.

The development of techniques to modulate the nonlinear coefficient of materials with micron-scale resolution opened new possibilities for frequency conversion of lasers. In particular, it allowed the creation of new mid-infrared coherent radiation sources, for example via difference frequency generation (DFG) [1–3] or optical parametric oscillation (OPO) [4]. Nonlinear frequency mixing is based on compact and efficient lasers, which presently exist mainly in the near infrared region, and the resulting sources are characterized by a wide tunability range and high spectral resolution. In the case of DFG, the wide range and continuous tuning is easily achieved, since the idler wavelength is determined by the pump and signal wavelengths, and only the conversion efficiency depends on the phase-matching conditions. Moreover, unlike in OPO, there is no threshold requirement for DFG.

During the last few years, methods for modulating the nonlinear coefficient in nonlinear materials were developed. With these techniques, the concept of quasi-phase-matching [5] could be realized, for example in ferroelectric crystals via the electric-field poling scheme. This technique was already successfully applied to LiNbO<sub>3</sub> [6], KTiOPO<sub>4</sub> (KTP) [7,8], LiTaO<sub>3</sub> [9], RbTiOAsO<sub>4</sub> (RTA) [10,11] and KTiOAsO<sub>4</sub> (KTA) [12] crystals.

In this paper, we report the development and results of a table-top room-temperature gas sensor, designed for high resolution sensitive absolute measurements of gases that exhibit absorption lines in the 3.1–3.75  $\mu\text{m}$  spectral range. The tunability of the spectrometer and its high spectral resolution are used to study entire vibrational bands as well as fine details within the absorption spectra of methane (CH<sub>4</sub>) and nitrous oxide (N<sub>2</sub>O).

## **2. Experimental setup**

The DFG experimental setup is shown in Fig. 1. It consists of two compact single-mode laser sources: a diode-pumped Nd:YAG laser at 1064.4 nm and an external cavity tunable diode laser near 1.55  $\mu\text{m}$  (tuning range  $\sim 100$  nm). The beams of the pump and signal lasers are combined collinearly using a dichroic beamsplitter and are focused onto the periodically poled nonlinear crystal.

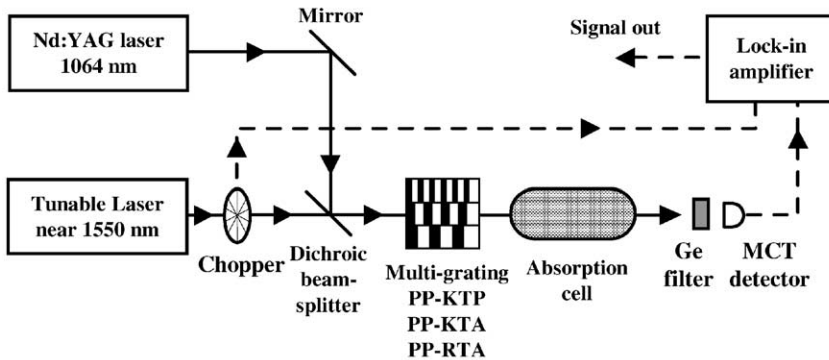


Fig. 1. Experimental setup for DFG of mid-IR radiation in periodically poled crystals of the KTP family. The absorption cell is used for spectroscopic measurements.

We used three different multi-grating periodically poled (PP) crystals of the KTP family in our spectrometer, namely: PP-KTP [1], PP-KTA [2] and PP-RTA [3]. Of these three crystals, KTP [13] is the most commonly used one and is commercially available from a variety of suppliers at a relatively low price. It exhibits a high damage threshold and is less sensitive to thermal sensing, compared to  $\text{LiNbO}_3$ . KTP is transparent over a wide wavelength range: 350–4000 nm. Unfortunately, it also exhibits significant absorption around  $\approx 3.3 \mu\text{m}$ . One of the important characteristics of the alkali metal titanyl arsenate crystals, such as KTA and RTA, is that in addition to maintaining most of the valuable properties of KTP, e.g. high damage threshold and low coercive field, they also lack the significant absorption that KTP exhibits around  $\approx 3.3 \mu\text{m}$ . Moreover, they enjoy a longer cutoff wavelength of  $\approx 5.3 \mu\text{m}$ , compared to  $\approx 4 \mu\text{m}$  in KTP [14,15]. While flux-grown KTP and KTA crystals should either be cooled to low temperature ( $\approx 170 \text{ K}$ ) [8] or pre-treated by chemical indiffusion of Rb ions [16], RTA crystals have been poled near room temperature without any pre-treatment [10]. Furthermore, since the poling field increases as the temperature decreases, the electric field required to pole RTA near room temperature is  $\approx 2.5 \text{ kV/mm}$  [10,11], less than half of that required for KTP and KTA at 170 K, and approximately an order of magnitude lower than that of  $\text{LiNbO}_3$  [17]. Owing to that, fairly thick samples ( $\approx 3 \text{ mm}$ ) have been periodically poled by electric field [18].

The grating periods were between 35.7 and 40.2  $\mu\text{m}$ , depending on the crystal, with a  $\sim 50\%$  duty cycle. In order to effectively generate the mid-IR coherent radiation, we use the largest element of the nonlinear coefficient tensor,  $d_{33}$ . The variety of crystals, as well as the multi-grating structure, enable us to generate widely tunable mid-IR coherent radiation between 3.1 and 3.75  $\mu\text{m}$ . The same technique may be used to generate coherent radiation up to an idler wavelength of  $\sim 5 \mu\text{m}$ , limited only by the transparency of the nonlinear crystal [15].

The generated mid-IR radiation is detected with a liquid-nitrogen-cooled HgCdTe detector that exhibits a relatively low noise-equivalent-power of  $\sim 1 \text{ pW}/\sqrt{\text{Hz}}$ . A

tilted uncoated germanium window is used to block the pump and signal beams from entering the detector. The signal beam is chopped at a rate of  $\sim 1.5$  kHz, and the idler is detected with a lock-in-amplifier. The wavelengths of the pump and signal lasers are measured using a wavemeter.

### 3. Spectroscopic measurements

In order to perform spectroscopic measurements, we use a 10-cm-long absorption cell with windows that are transparent in the mid-IR. To demonstrate the use of our laser spectrometer and to test its performance, we measure the absorption spectra of methane ( $\text{CH}_4$ ) and nitrous oxide ( $\text{N}_2\text{O}$ ) at  $\sim 3.3$ – $3.5$   $\mu\text{m}$ . The absorption cell is evacuated to a vacuum level of  $\sim 50$  mTorr by a rotation vacuum pump, and then filled with the inspected gas. The pressure of the gas in the absorption cell is monitored on-line throughout the experiment with a vacuum gauge. The wide tunability of the spectrometer enables us to cover entire vibrational bands of methane and of nitrous oxide. The high spectral resolution ( $\sim 1$  MHz) is useful for investigating hyperfine components of a single rotational transition.

#### 3.1. Methane ( $\text{CH}_4$ )

We measure the absorption spectrum of methane near the  $\nu_3$ -band at 3.3  $\mu\text{m}$ , which is one of its four fundamental vibration bands. Fig. 2a shows our measurements of this vibration band (performed with PP-KTP). Note the residual envelope when measuring in vacuum which is due to the wavelength-dependent efficiency curve of the nonlinear device.

The generated coherent source had a narrow linewidth ( $\sim 1$  MHz), which enables us to perform high spectral resolution measurements. For example, the splitting of the P(6) line into 6 hyperfine components is clearly seen in Fig. 2b. Further magnification reveals details within one absorption line, and enables us to investigate, for example, its pressure broadening (Fig. 2c). Fig. 3a shows a scan of the same P(6) hyperfine splitting, performed by Barnes et al. using FTIR spectrometer [19]. This scan was performed with a spectrometer that had a much lower spectral resolution compared to our DFG source (about 500 MHz compared to  $\sim 1$  MHz). Consequently, it can be seen that lines that are not fully resolved in [19] are clearly separated in our measurement, see Fig. 3b. Note that the main broadening mechanism in the measurements shown in Fig. 3 is the Doppler broadening, having a full width at half maximum linewidth of  $\sim 280$  MHz, which is of the same order as the FTIR spectrometer resolution. Therefore, the resolution is limited also by the absorption linewidth. However, the narrow linewidth of the DFG-based spectrometer can be of great importance when performing sub-Doppler [20] or low-pressure measurements.

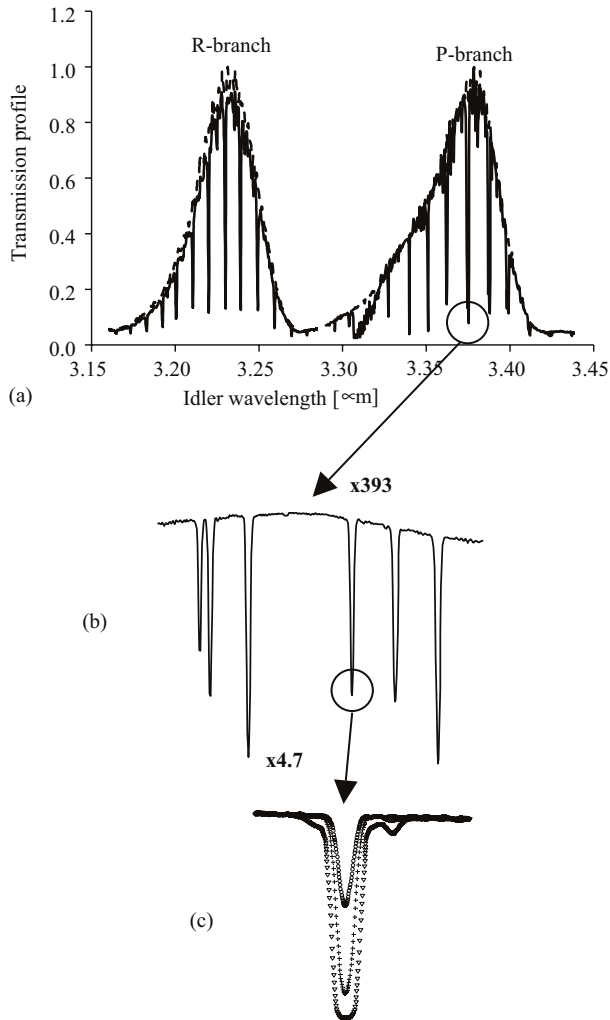


Fig. 2. Measurements of the  $\nu_3$ -band of pure methane using DFG in a periodically poled KTP crystal. (a) R-branch and P-branch spectrum of methane (dashed curve—vacuum, solid curve—78 Torr). (b) High resolution scan of P(6) group (0.75 Torr). (c) Investigation of a single line within the P(6) group in various pressures (circles—0.6 Torr, crosses—1.3 Torr, triangles—4.5 Torr).

The lineshape of an absorption line is generally given by the Voigt profile [21]:

$$V(x) = \frac{y}{\alpha_D} \sqrt{\frac{\ln 2}{\pi^3}} \int_{-\infty}^{\infty} \frac{\exp(-t^2)}{y^2 + (x - t)^2} dt \quad (\text{Hz}^{-1}), \quad (1)$$

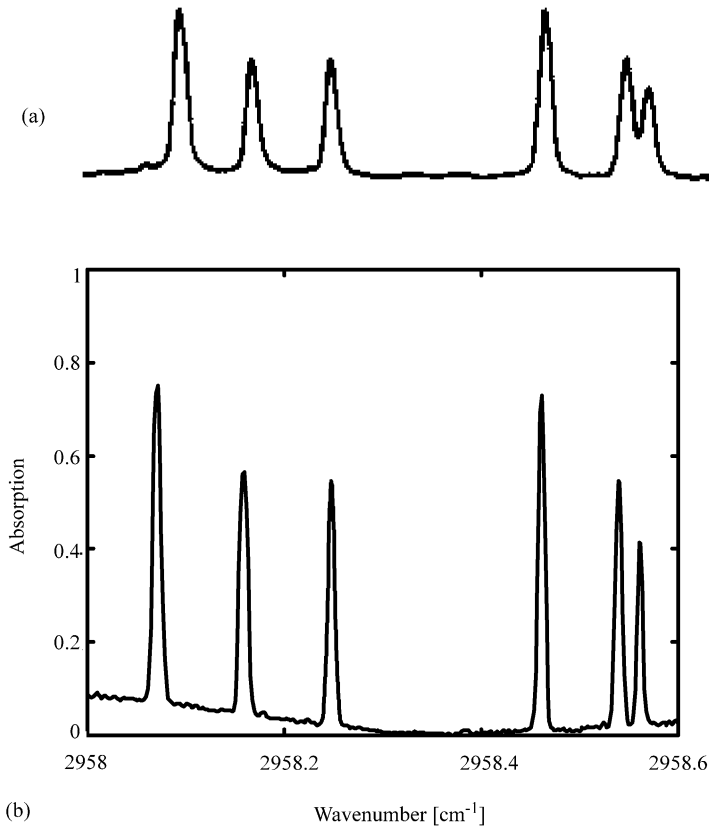


Fig. 3. A scan of the P(6) transition. (a) Performed by Barnes et al. [19] using FTIR spectrometer (spectral resolution  $\sim 500$  MHz) [19]. (b) Performed using our spectrometer.

where  $y$  represents the ratio of Lorentz to Doppler half-widths and is given by

$$y = \frac{\alpha_L}{\alpha_D} \sqrt{\ln 2}, \quad (2)$$

where  $\alpha_D$  is the Doppler half-width, given by

$$\alpha_D = 3.581 \times 10^{-7} v_0 \sqrt{\frac{T}{m}} \text{ (Hz)}, \quad (3)$$

and  $\alpha_L$  is the Lorentz half-width (in Hz).  $v_0$  is the frequency at the center of the line (in Hz),  $T$  is the temperature (in Kelvin),  $m$  is the molecular mass (in atomic mass units) and  $x$  is the distance from this frequency scaled in units of Doppler width:

$$x = \frac{\nu - \nu_0}{\alpha_D} \sqrt{\ln 2}. \quad (4)$$

The absorption coefficient,  $\alpha$ , is given by

$$\alpha(x) = 3 \times 10^6 V(x) S C_{\text{gas}} \text{ (m}^{-1}\text{)}, \quad (5)$$

Table 1

Line strengths and air-pressure broadening coefficients of the 6 hyperfine components of the P(6) line of methane (taken from the HITRAN database [22]). Central wavelength measurement performed using our experimental setup

Line	Central wavenumber (cm <sup>-1</sup> )	Line strength (cm <sup>2</sup> cm <sup>-1</sup> )	Air-pressure broadening coefficient (cm <sup>-1</sup> atm <sup>-1</sup> )
<i>A</i> <sub>1</sub>	2958.074	1.06 × 10 <sup>-19</sup>	0.0560
<i>F</i> <sub>1</sub>	2958.168	6.32 × 10 <sup>-20</sup>	0.0617
<i>F</i> <sub>2</sub>	2958.258	6.28 × 10 <sup>-20</sup>	0.0645
<i>A</i> <sub>2</sub>	2958.471	1.07 × 10 <sup>-19</sup>	0.0638
<i>F</i> <sub>2</sub>	2958.553	6.389 × 10 <sup>-20</sup>	0.0543
<i>E</i>	2958.579	4.269 × 10 <sup>-20</sup>	0.0625

where  $S$  is the line strength (in cm<sup>2</sup> cm<sup>-1</sup>) and  $C_{\text{gas}}$  is the concentration of the gas (in m<sup>-3</sup>), which can be calculated from the ideal gas law and is given by

$$C_{\text{gas}} = 101325 \frac{P_{\text{gas}} \text{NA}}{RT} \text{ (m}^{-3}\text{)}, \quad (6)$$

where  $P_{\text{gas}}$  is the gas partial pressure (in atm),  $\text{NA} = 6.022 \times 10^{23}$  (mol<sup>-1</sup>) is Avogadro's number and  $R = 8.3144$  (JK<sup>-1</sup> mol<sup>-1</sup>) is the universal gas constant. Combining Eqs. (5) and (6) we get

$$\alpha(x) = 3.04 \times 10^{11} V(x) S \frac{P_{\text{gas}} \text{NA}}{RT} \text{ (m}^{-1}\text{)}. \quad (7)$$

The transmission,  $T$ , is simply

$$T(x) = \exp[-\alpha(x)L], \quad (8)$$

where  $L$  is the length of the absorption cell (in m). The line strengths and the air-pressure broadening coefficients of these lines are taken from the HITRAN database [22], see Table 1. The central wavenumbers of these absorption lines were calculated from the measured wavenumbers of the Nd:YAG and external cavity lasers. We use the data from the HITRAN database as well as the theoretical Voigt profile to fit the transmission measurements near the splitting of the P(6) line for methane mixed with air (total pressure 29 Torr; 5% Methane = 1.45 Torr). Both the theoretical curve and the measured transmission are shown in Fig. 4, and it can be seen that there is excellent agreement between them.

For a line with well-known parameters, this theoretical model enables to measure concentrations of the gas in ambient air. For weak absorptions

$$\exp[-\alpha_{\text{max}}L] = 1 - \alpha_{\text{max}}L, \quad (9)$$

where  $\alpha_{\text{max}}$  is the absorption coefficient at the central frequency. Assuming that SNR of 1 is sufficient for detection, and with a minimum detectable change in the transmission,  $\Delta T_{\text{min}}$ , we get:

$$\alpha_{\text{max}}L = \Delta T_{\text{min}}. \quad (10)$$

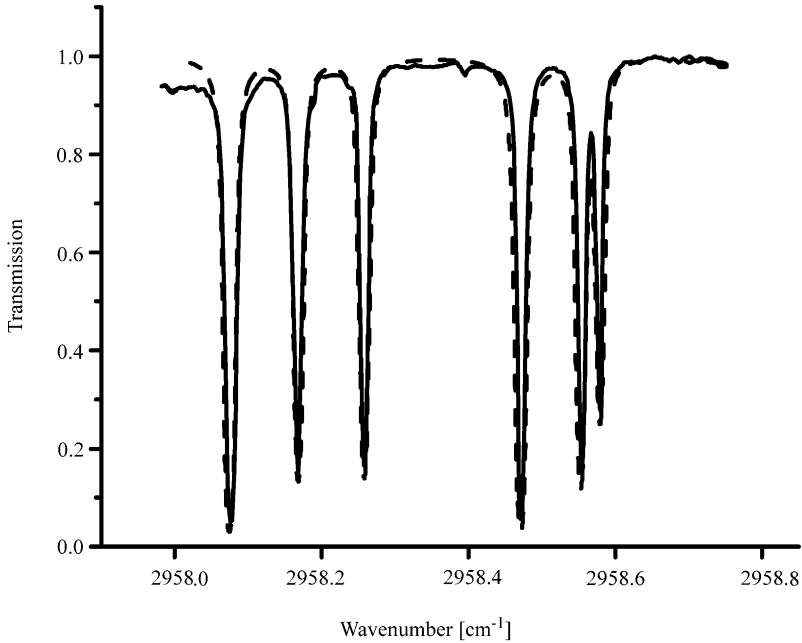


Fig. 4. A scan of the P(6) transition for methane mixed with air (methane pressure: 1.45 Torr, total pressure: 29 Torr). The solid curve is measured with a PP-KTP based DFG source. The dashed curve is calculated theoretically based on the Voigt profile and lines parameters taken from the HITRAN database.

Using Eqs. (5) and (10) and the relation between the Voigt profile value at the central frequency and the Lorentz half-width:

$$V_{\max} = \frac{1}{\pi\alpha_L} \text{ (Hz}^{-1}\text{)}, \quad (11)$$

we can calculate the minimum detectable concentration of methane,  $C_{\min}$ :

$$C_{\min} = 10^4 \frac{\pi\Delta T_{\min} k_{\text{gas-air}} P_{\text{total}}}{LS} \text{ (m}^{-3}\text{)}, \quad (12)$$

where  $k_{\text{gas-air}}$  is the air-pressure broadening coefficient (in  $\text{cm}^{-1} \text{atm}^{-1}$ ) and  $P_{\text{total}}$  is the total pressure (in atm). Since the total concentration of molecules (air + methane) is given by the ideal gas law:

$$C_{\text{total}} = 101325 \frac{P_{\text{total}} NA}{RT} \text{ (m}^{-3}\text{)}, \quad (13)$$

it follows that the fractional concentration of methane is

$$\frac{C_{\min}}{C_{\text{total}}} = 0.0987 \frac{\pi\Delta T_{\min} k_{\text{gas-air}} RT}{LS NA}. \quad (14)$$

For the P(6) transition, typical values are:  $S \approx 10^{-19} \text{ cm}$  and  $k_{\text{CH}_4\text{-air}} \approx 0.06 \text{ cm}^{-1} \text{atm}^{-1}$ . Since neither the optical elements nor the crystal were anti-reflection



coated, the measurements exhibited significant etalon effects, thus  $\Delta T_{\min} \approx 0.01$ . Therefore, the minimum detectable fractional concentration of methane at room temperature is  $\approx 75$  ppm (parts per million). By using coated optics and crystals to reduce the etalon effects, as well as more sensitive detection schemes such as FM spectroscopy,  $\Delta T_{\min}$  can be lowered to  $10^{-5}$  [23]. Furthermore, the effective absorption length can be increased to the range of 30–100 m using a multipass cell. Thus, the sensitivity can be significantly improved to the ppb (parts per billion) range.

### 3.2. Nitrous oxide ( $N_2O$ )

We measure the absorption spectrum of nitrous oxide near  $3.6 \mu\text{m}$ . The stronger lines are for the vibrational transition  $0000 \rightarrow 0111$ , and some weaker lines are for the  $0110 \rightarrow 0221$  and the  $0110 \rightarrow 0201$  overtone transitions. Fig. 5 shows our measurements of these lines (performed with PP-KTA) for two nitrous oxide pressures. Note that the line strength of these lines is approximately lower by two to three orders of magnitude compared to that of methane. As with methane, the narrow linewidth of the generated radiation ( $\sim 1$  MHz) enables us to perform measurements with high spectral resolution. Fig. 6 shows the effect of pressure broadening on a single transition at  $2816.449 \text{ cm}^{-1}$ . This line can be identified in the HITRAN database, and its assignment is:  $0000 \rightarrow 0111$ , R(23).

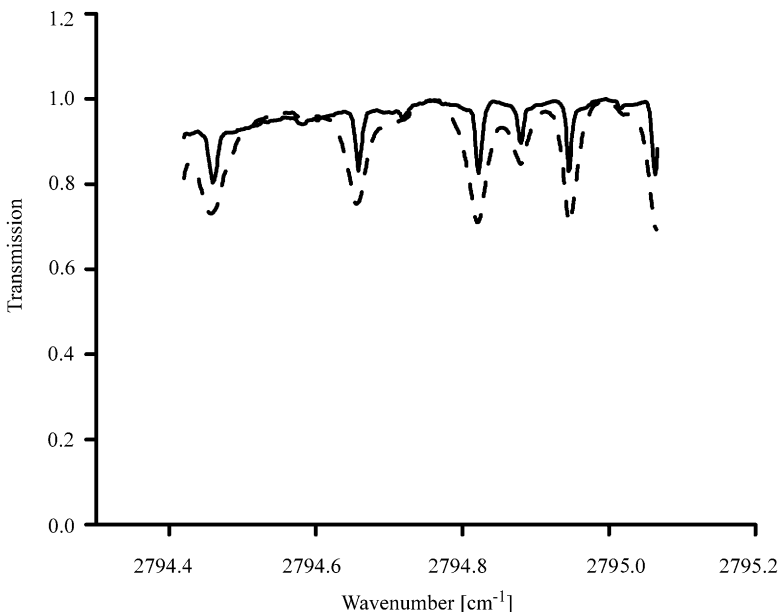


Fig. 5. Absorption spectrum of pure nitrous oxide near  $3.5 \mu\text{m}$  for several pressures (solid—18 Torr; dashed—147 Torr). The measurements were performed with a PP-KTA based DFG source.

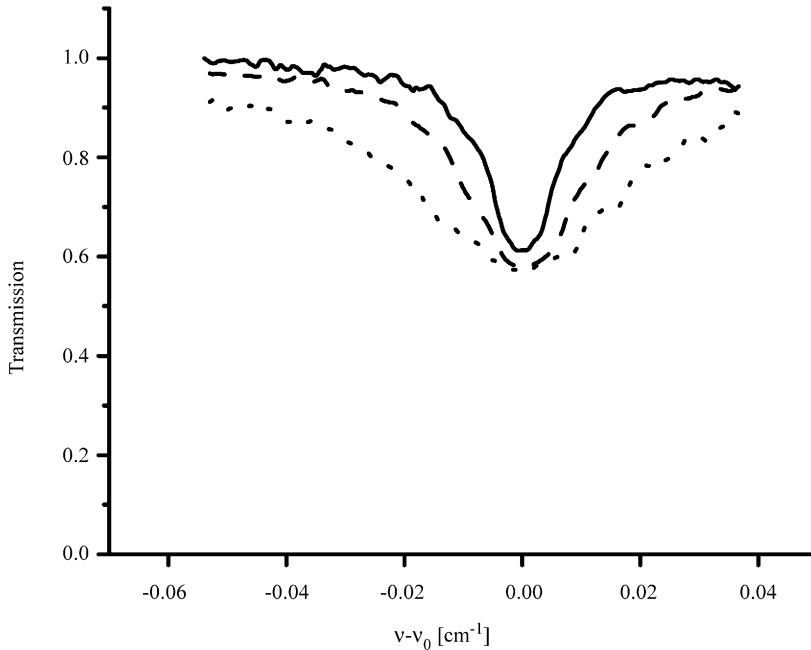


Fig. 6. The effect of pressure broadening on a single absorption line of nitrous oxide at  $2816.449\text{ cm}^{-1}$ ,  $0000 \rightarrow 0111$ , R(23) (solid—28 Torr, dashed—58 Torr, dotted—109 Torr).

#### 4. Summary and conclusions

In conclusion, we have constructed a compact room-temperature mid-infrared laser spectrometer, based on quasi-phase matched DFG in periodically poled ferroelectric crystals of the KTP family. The spectrometer has been designed for high resolution sensitive measurements of gases that have absorption lines in the  $3.1\text{--}3.75\text{ }\mu\text{m}$  spectral range. The tunability of this spectrometer and its high spectral resolution ( $\sim 1\text{ MHz}$ ) enabled us to study entire vibrational bands, as well as fine details within the absorption spectra of methane ( $\text{CH}_4$ ) and nitrous oxide ( $\text{N}_2\text{O}$ ). Naturally, it can be used as a gas sensor for any other gas which absorbs in the above mentioned spectral range, where most environmentally important gases and pollutants exhibit their strongest absorption lines.

We have shown that this compact and robust source is suitable for sensitive quantitative concentration measurements. With a rather short absorption cell ( $\sim 10\text{ cm}$ ) we have demonstrated a minimum detectable concentration of 75 ppm. The sensitivity can be further improved to the ppb range, for example by using a longer absorption path length or by applying a proper anti-reflection coating to the optical elements.

Further improvements in sensitivity can be attained by using advanced and more sophisticated spectroscopy techniques, instead of the simple absorption spectroscopy

scheme that was used here. Examples for such techniques are: FM sideband spectroscopy [23,24] and intra-cavity ring down spectroscopy [25].

Recently, we have proposed novel quasi-periodic nonlinear mixers [26] that exhibit simultaneous phase-matching for several nonlinear interactions. A laser spectrometer based on such mixers will have the advantage of covering several different spectral ranges, which are determined by the conversion efficiency curve. If the mixer is designed to have a conversion efficiency curve that is proportional to the relative strength of the absorption profile of a specific gas, it can act as a discriminator against other gases, which absorb in the same spectral range.

## Acknowledgements

The authors wish to thank Prof. Gil Rosenman and Mr. Pavel Urenski for preparing the periodically poled crystals that were used in the reported research. Keren Fradkin-Kashi is an Eshkol Scholar from the Israeli ministry of science, culture and sport. The research was partly funded by the Israeli ministry of science, culture and sport and by the German-Israeli Foundation for scientific research and development.

## References

- [1] Fradkin K, Arie A, Skliar A, Rosenman G. Tunable midinfrared source by difference frequency generation in bulk periodically poled KTiOPO<sub>4</sub>. *Appl Phys Lett* 1999;74(7):914–6.
- [2] Fradkin-Kashi K, Arie A, Urenski P, Rosenman G. Mid-infrared difference frequency generation in periodically poled KTiOAsO<sub>4</sub> and application to gas sensing. *Opt Lett* 2000;25(10):743–5.
- [3] Fradkin-Kashi K, Arie A, Urenski P, Rosenman G. Characterization of optical and nonlinear properties of periodically poled RbTiOAsO<sub>4</sub> in the mid-infrared range via difference-frequency generation. *Appl Phys B* 2000;71(2):251–5.
- [4] Weise DR, Ströbner U, Peters A, Mlynek J, Schiller S, Arie A, Skliar A, Rosenman G. Continuous-wave 532-nm-pumped singly resonant optical parametric oscillator with periodically poled KTiOPO<sub>4</sub>. *Opt Comm* 2000;184(1–4):329–33.
- [5] Armstrong JA, Bloembergen N, Ducuing J, Pershan PS. Interactions between light waves in a nonlinear dielectric. *Phys Rev* 1962;127(6):1918–39.
- [6] Yamada M, Nada N, Saitoh M, Watanabe K. 1st order quasi-phase matched LiNbO<sub>3</sub> wave-guide periodically poled by applying an external-field for efficient blue 2nd-harmonic generation. *Appl Phys Lett* 1993;62(5):435–6.
- [7] Chen Q, Risk WP. Periodic poling of KTiOPO<sub>4</sub> using an applied electric-field. *Electron Lett* 1994;30(18):1516–7.
- [8] Rosenman G, Skliar A, Eger D, Oron M, Katz M. Low temperature periodic electrical poling of flux-grown KTiOPO<sub>4</sub> and isomorphic crystals. *Appl Phys Lett* 1998;73(25):3650–2.
- [9] Zhu SN, Zhu YY, Yang ZJ, Wang HF, Zhang ZY, Hong JF, Ge CZ. Second-harmonic generation of blue light in bulk periodically poled LiTaO<sub>3</sub>. *Appl Phys Lett* 1995;67(3):320–2.
- [10] Karlsson H, Laurell F, Henriksson P, Arvidsson G. Frequency doubling in periodically poled RbTiOAsO<sub>4</sub>. *Electron Lett* 1996;32(6):556–7.
- [11] Hu ZW, Thomas PA, Webjorn J, Loiacono GM. Domain inversion in RbTiOAsO<sub>4</sub> using electric field poling. *J Phys D Appl Phys* 1996;29(6):1681–4.

- [12] Rosenman G, Skliar A, Findling Y, Urenski P, Englander A, Thomas PA, Hu ZW. Periodically poled KTiOAsO<sub>4</sub> crystals for optical parametric oscillation. *J Phys D Appl Phys* 1999;32(14):L49–52.
- [13] Bierlein D, Vanherzeele H. Potassium titanyl phosphate: properties and new applications. *J Opt Soc Am B* 1989;6(4):622–33.
- [14] Bosenberg WR, Cheng LK, Bierlein JD. Optical parametric frequency conversion properties of KTiOAsO<sub>4</sub>. *Appl Phys Lett* 1994;65(22):2765–7.
- [15] Cheng LK, Bierlein JD. KTP and isomorphs—recent progress in device and material development. *Ferroelectrics* 1993;142(1–2):209–28.
- [16] Karlsson H, Laurell F. Electric field poling of flux grown KTiOPO<sub>4</sub>. *Appl Phys Lett* 1997;71(24):3474–6.
- [17] Myers LE, Eckardt RC, Fejer MM, Byer RL, Bosenberg WR, Pierce JW. Quasi-phase-matched optical parametric oscillators in bulk periodically poled LiNbO<sub>3</sub>. *J Opt Soc Am B* 1995;12(11):2102–16.
- [18] Karlsson H, Olson M, Arvidsson G, Laurell F, Bader U, Borsutzky A, Wallenstein R, Wickstrom S, Gustafsson M. Nanosecond optical parametric oscillator based on large-aperture periodically poled RbTiOAsO<sub>4</sub>. *Opt Lett* 1999;24(5):330–2.
- [19] Barnes WL, Susskind J, Hunt RH, Plyler EK. Measurement and analysis of the  $\nu_3$  band of methane. *J Chem Phys* 1972;56(10):5160–72.
- [20] Mazzotti D, De Natale P, Giusfredi G, Fort C, Mitchell JA, Hollberg L. Saturated-absorption spectroscopy with low-power difference frequency radiation. *Opt Lett* 2000;25(5):350–2.
- [21] Armstrong BH. Spectrum line profiles: the Voigt function. *J Quant Spectrosc Radiat Transfer* 1967;7(1):61–88.
- [22] Rothman LS, Rinsland CP, Goldman A, Massie ST, Edwards DP, Flaud JM, Perrin A, Camy-Peyret C, Dana V, Mandin JY, Schroeder J, McCann A, Gamache RR, Wattson RB, Yoshino K, Chance KV, Jucks KW, Brown LR, Nemtchinov V, Varanasi P. The HITRAN molecular spectroscopic database and HAWKS (HITRAN Atmospheric Workstation): 1996 edition. *J Quant Spectrosc Radiat Transfer* 1998;60(5):665–710.
- [23] Bjorklund GC. Frequency-modulation spectroscopy: a new method for measuring weak absorptions and dispersions. *Opt Lett* 1980;5(1):15–7.
- [24] Hall JL, Hollberg L, Baer T, Robinson HG. Optical heterodyne saturation spectroscopy. *Appl Phys Lett* 1981;39(9):680–2.
- [25] Inbar E, Arie A. High-sensitivity CW Fabry-Perot enhanced spectroscopy of CO<sub>2</sub> and C<sub>2</sub>H<sub>2</sub> using a 1064-nm Nd:YAG laser. *Appl Phys B* 1999;68(1):99–105.
- [26] Fradkin-Kashi K, Arie A. Multiple-wavelength quasi-phase-matched nonlinear interactions. *IEEE J Quantum Electron* 1999;35(11):1649–56.